# Atmospheric Pressure Plasma Enhanced Synthesis of Flame Retardant Cellulosic Materials

**Vladimir Totolin,[1] Majid Sarmadi,[1,2,3] Sorin O. Manolache,[3] Ferencz S. Denes[3,4]**

[1]*Materials Science Program, University of Wisconsin-Madison, Wisconsin 53706*
[2]*School of Human Ecology, University of Wisconsin-Madison, Wisconsin 53706*
[3]*Center for Plasma-Aided Manufacturing, Madison, Wisconsin 53706*
[4]*Department of Biological Systems Engineering, University of Wisconsin, Madison, Wisconsin 53706*

Received 14 October 2009; accepted 16 December 2009
DOI 10.1002/app.31987
Published online 2 March 2010 in Wiley InterScience (www.interscience.wiley.com).

**ABSTRACT:** Flame retardant cellulosic materials have been produced using a silicon dioxide ($SiO_2$) network coating. $SiO_2$ network armor was prepared through hydrolysis and condensation of the precursor tetraethyl orthosilicate (TEOS), prior coating the substrates, and was cross linked on the surface of the substrates using atmospheric pressure plasma (APP) technique. Because of protection effects of the $SiO_2$ network armor, the cellulosic based fibers exhibit enhanced thermal properties (characterized by TGA and DSC) and improved flame retardant (proven by ASTM D1230-99). Furthermore, the surface analysis (XPS and SEM) confirmed the presence of the $SiO_2$ network attached to the substrates even after intense ultrasound washes. © 2010 Wiley Periodicals, Inc. J Appl Polym Sci 117: 281–289, 2010

**Key words:** flame retardant; cellulosic fibers; atmospheric pressure plasma; $SiO_2$; coating; crosslinking; TEOS

## INTRODUCTION

Natural polymers are a crucial part of today's life; they can be found nearly everywhere. Nowadays, natural polymer materials are having a comeback due to their specific properties (i.e., excellent mechanical properties, biodegradable, sustainable, etc.). However, one weak aspect of natural polymer materials compared with other materials is that they are combustible. Among them, cellulosic textiles are probably the most flammable[1] with cotton being the most commonly used of all textile fibers. Thus, the majority of polymer-containing end-products (e.g., cables, carpets, furniture cabinets, etc.) must have a satisfactory degree of fire resistance to ensure public safety from fire.

Silicone materials have been produced commercially since the beginning of the 1940s. Over the past 60 years, silicone materials have grown into a billion-dollar industry, and are used in many applications in civil engineering, construction building, electrical, transportation, aerospace, defense, textiles, and cosmetics industries.[2] The main structural elements of siloxanes have a direct or indirect influence on their stability at elevated temperatures, including: inherent strength of the Si—O bond and pronounced flexibility of the siloxane — $[Si—O]_x$— chain segments.[3]

Siloxanes have comparatively low heat release rates (HRR), minimal sensitivity to external heat flux, and low yields of carbon monoxide release.[4] They also show a slow burning rate without a flaming drip and when pure, no emissions of toxic smokes. Based on these fire properties, silicones offer significant advantages for flame retardant (FR) applications. Unlike organic polymers, silicones exposed to elevated temperatures under oxygen leave behind a silica residue. Its shielding effects provide some of the fundamentals for the development of silicone-based fire retardants. Silica residue serves as an "insulating blanket," which acts as a mass transport barrier delaying the volatilization of decomposition products. Therefore, it reduces the amount of volatiles available for burning in the gas phase, and thus the amount of heat that feeds back to the polymer surface. The silica residue also serves to insulate the underlying polymer surface from incoming external heat flux.[5]

It is believed that silicone-based flame retardants (FRs) used for synthetic or natural polymers act in two basic ways: By thermal quenching (endothermic decomposition of the FR) and by forming a protective coating (liquid or char barrier).[6–16] Because of increased market and societal demand for materials that can be processed by environmentally friendly

*Correspondence to:* M. Sarmadi (majidsar@wisc.edu).
Contract grant sponsor: US Department of Agriculture; contract grant number: S-1026.

methods, new and innovative production techniques are needed. These have led to further development of alternative physicochemical processing methods. In this field, plasma technology shows distinct advantages because it is environmentally friendly, and surface properties of even inert materials can be easily modified.[17]

This article discusses the improvement of FR properties of cotton using a sol-gel process in conjunction with atmospheric pressure plasma (APP) treatments.

## EXPERIMENTAL

### Materials

Bleached Desized Cotton Print Cloth (78× 76), weight = 102 g/m$^2$ was purchased from Test Fabrics and cut in 2 × 6″ samples. Tetraethyl orthosilicate (TEOS) solution (98 wt %) was purchased from Sigma Aldrich Chemicals.

### Procedure

The overall scheme of functionalizing cotton surfaces is shown in Figure 1.

Samples were Soxhlet extracted in a toluene/ethanol mixture (1 : 2 ratios) for 24 h in order the remove the impurities from fibers, then dried overnight in a vacuum oven at 30 mmHg, at room temperature. The FR coating was silica ($SiO_2$) generated through hydrolysis and condensation of the precursor TEOS, prior coating the substrates [eq. (1)].

$$Si(OC_2H_5)_4 + 2H_2O \longrightarrow SiO_2 + 4C_2H_5OH \qquad (1)$$

The precursor concentrations (10, 20, 30, and 40 wt %) were chosen according to a statistical design of the experiments (Design-Expert Software). The samples were dip coated in solution at different temperatures (20–80°C) for 2 h that resulted in different $SiO_2$ concentrations (3, 6, 9, and 11.5 wt %) on the cotton substrates. After soaking the samples were dried in a vacuum oven overnight at room temperature and then were exposed to atmospheric pressure plasma treatments. To remove the nonreacted particles the samples were washed 30 min in deionized (DI) water using an ultrasound bath after the plasma treatment. Three washings were performed for each batch.

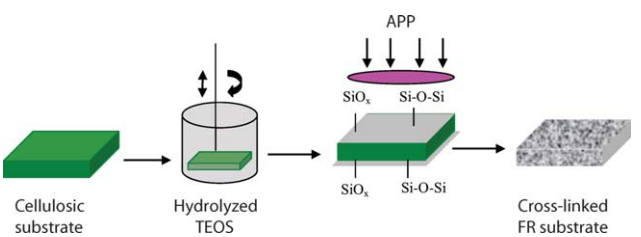


**Figure 1** Scheme of cotton's dip-coating process. [Color figure can be viewed in the online issue, which is available at www.interscience.wiley.com.]

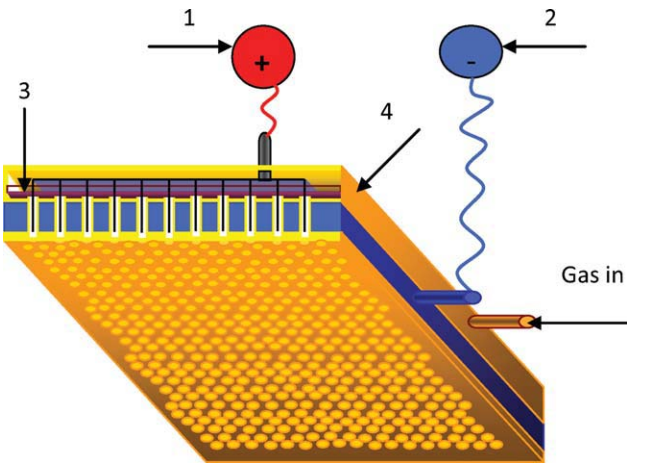


**Figure 2** Scheme of array electrode reactor (AER). 1, 2: Metallic electrodes; 3: Distribution grid; 4: Ceramic coating. [Color figure can be viewed in the online issue, which is available at www.interscience.wiley.com.]

### Atmospheric plasma reactor

Atmospheric pressure plasma treatments were carried out in an Array Electrode Reactor (AER) containing an array of approximate 250 tubular reactors, each with a diameter of 2 mm.[18] The reactor is equipped with a high voltage power supply and the following plasma parameters were used: 40–100 W RF Power, 2–8 min exposure time. The gas used was air at a flow rate of 498 sccm. A scheme of the reactor is presented in Figure 2.

### 45° angle flammability test (ASTM D1230-99)

The plasma-treated and washed samples were dried in vacuum oven overnight at the room temperature and then tested for flammability with a 45° angle Auto-Flame chamber. This test is design to measure and describe the behavior of natural or synthetic fabrics in response to heat and flame under controlled lab conditions. Samples were mounted in a frame and held in an auto-flame chamber at an angle of 45°. A standardized flame was applied to the substrate's surface near its lower end for 1 s. The flame traveled up the length of the fabric to a trigger string, which dropped a weight to stop the timer when the sample was burned through. The time required for the flame to travel the length of the fabric and break the trigger string was recorded, as well as the fabric's ignition time.[19] Five samples for each treatment were tested and the results were averaged. For further confirmation of these results, the tests have been duplicated.

**TABLE I**
**The Experimental Treatment Parameters and Burning Spread Time**

| Concentration (%) | Power (W) | Time (s) | Temperature (°C) | Burning time (s) | Mass deposited (%) |
|---|---|---|---|---|---|
| 0 | 0 | 0 | 0 | 9.00 | 0 |
| 20 | 50 | 3.5 | 35 | 25.25 | 12.04 |
| 40 | 50 | 3.5 | 35 | 30.80 | 24.10 |
| 20 | 80 | 3.5 | 35 | 26.30 | 7.73 |
| 40 | 80 | 3.5 | 35 | 28.63 | 22.42 |
| 20 | 50 | 6.5 | 35 | 24.00 | 9.15 |
| 40 | 50 | 6.5 | 35 | 30.10 | 25.17 |
| 20 | 80 | 6.5 | 35 | 24.40 | 7.22 |
| 40 | 80 | 6.5 | 35 | 31.20 | 24.57 |
| 20 | 50 | 3.5 | 65 | 28.25 | 14.74 |
| 40 | 50 | 3.5 | 65 | 31.45 | 30.12 |
| 20 | 80 | 3.5 | 65 | 29.75 | 13.32 |
| 40 | 80 | 3.5 | 65 | 27.60 | 26.08 |
| 20 | 50 | 6.5 | 65 | 23.50 | 9.37 |
| 40 | 50 | 6.5 | 65 | 32.15 | 27.30 |
| 20 | 80 | 6.5 | 65 | 23.75 | 10.84 |
| 40 | 80 | 6.5 | 65 | 28.35 | 26.88 |
| 10 | 70 | 5.0 | 50 | 11.95 | 6.19 |
| 30 | 40 | 5.0 | 50 | 27.75 | 16.02 |
| 30 | 100 | 5.0 | 50 | 29.15 | 17.12 |
| 30 | 70 | 2.0 | 50 | 28.15 | 19.32 |
| 30 | 70 | 8.0 | 50 | 27.75 | 16.02 |
| 30 | 70 | 5.0 | 20 | 29.70 | 17.73 |
| 30 | 70 | 5.0 | 80 | 27.10 | 22.25 |
| 30 | 70 | 5.0 | 50 | 29.70 | 17.73 |
| 30 | 70 | 5.0 | 50 | 32.45 | 20.05 |
| 30 | 70 | 5.0 | 50 | 30.25 | 19.48 |
| 30 | 70 | 5.0 | 50 | 32.45 | 20.05 |
| 30 | 70 | 5.0 | 50 | 31.20 | 17.29 |
| 30 | 70 | 5.0 | 50 | 32.45 | 20.05 |

### Thermo gravimetric analysis (TGA)

TGA measures weight changes in a material as a function of temperature (or time) under a controlled atmosphere. The samples were exposed to TGA analysis using a TGA Q500 from TA Instruments to evaluate their thermal stability. The samples were

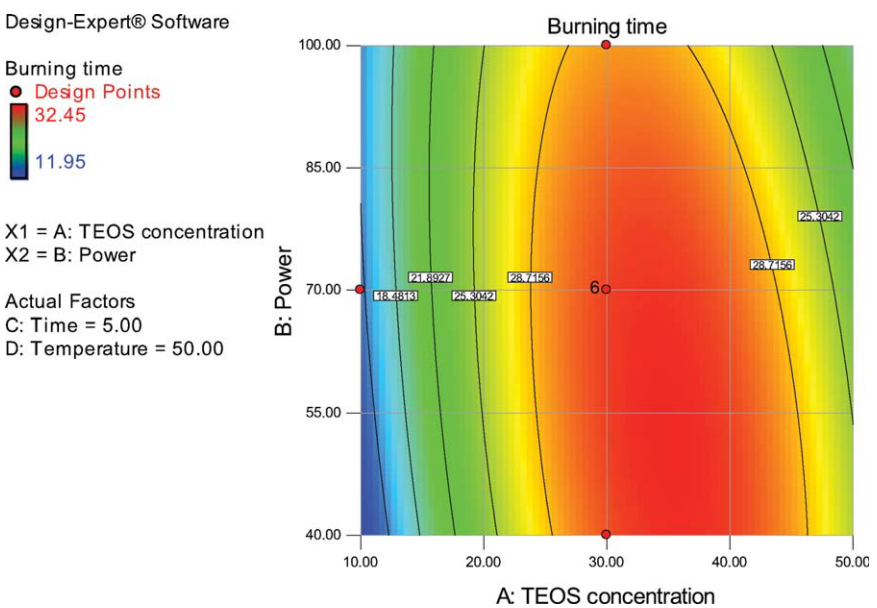


**Figure 3** Contour diagram for the response surface of burning spread time (s) versus RF power (W) and TEOS concentration (wt %). [Color figure can be viewed in the online issue, which is available at www.interscience.wiley.com.]

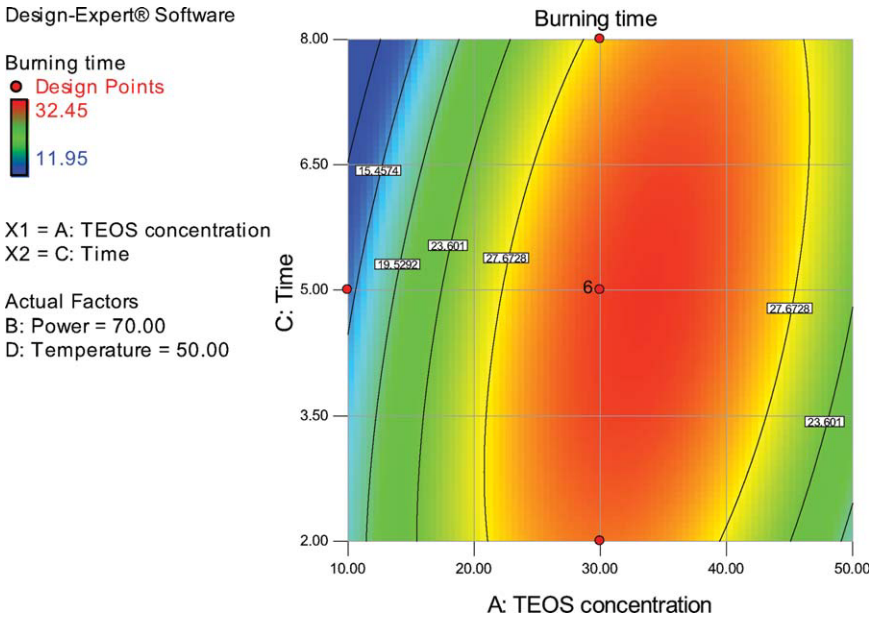


**Figure 4** Contour diagram for the response surface of burning spread time (s) versus plasma exposure time (min) and TEOS concentration (wt %). [Color figure can be viewed in the online issue, which is available at www.interscience.wiley.com.]

placed into the device under nitrogen blanket in the temperature range between 25°C and 700°C at a heating rate of 10°C/min.

### Differential scanning calorimeter (DSC)

DSC was used to evaluate the changes in thermal behavior of control and modified cotton using a Q100 Modulated DSC instrument from TA Instruments. The analysis were carried out under nitrogen atmosphere in the temperature range of 20–500°C using a heating rate of 10°C/min.

### Surface characterization

X-ray photoelectron spectroscopy (XPS)

A Perkin-Elmer Physical Electronics Phi 5400 Small Area Spectrometer (Mg source; 15 kV; 300 W; pass

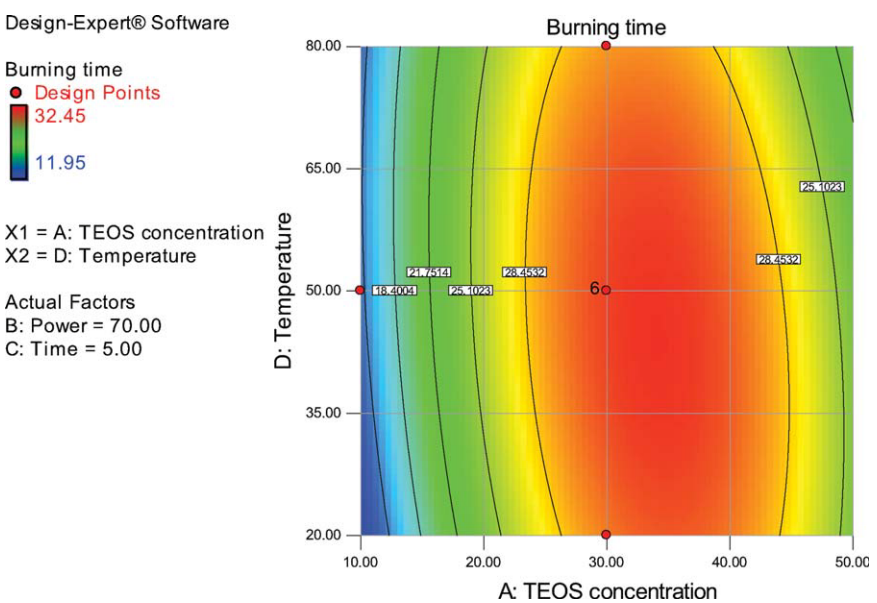


**Figure 5** Contour diagram for the response surface of burning spread time (s) versus solution temperature (°C) and TEOS concentration (wt %). [Color figure can be viewed in the online issue, which is available at www.interscience.wiley.com.]

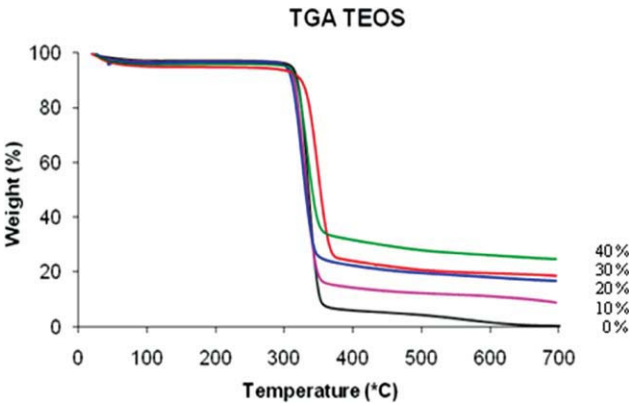


**Figure 6** TGA diagram of control versus plasma-modified samples. [Color figure can be viewed in the online issue, which is available at www.interscience.wiley.com.]

energy = 89.45 eV) was used for the XPS analysis. Both 15° and 45° take-off angles were used. Survey and high resolution (HR) scans were performed for core level evaluations. The curve fitting of the HR peaks were done using Gaussian algorithm.

### Scanning electron microscope (SEM)

To characterize the morphology of samples' surfaces as well as the uniformity of the coatings, the samples were analyzed with a LEO DSM 1530 FE Scanning Electron Microscope. The magnification used was 20,000×.

## RESULTS AND DISCUSSIONS

### 45° angle flammability test

The experimental parameters and the results from burning spread time of the samples are presented in Table I. It can be observed that 30 (wt %) concentrations of the precursor and medium RF power (70 W) led to longer burning time spread for the treated samples in comparison to control (non-treated) ones. The difference in burning time spread was about twice longer for concentrations as high as 20 wt % and more than three times longer for 30 and 40 wt % of TEOS.

### Investigation of APP parameters

To investigate the influence of experimental parameter-space on the process and select the optimal conditions, a statistical design of experiments was conducted. Four parameters were taken into consideration: TEOS concentration (wt %), RF power (W), plasma exposure time (min) and temperature of the solution (°C) during the coating process. The contour diagrams (Figs. 3–5) present the response

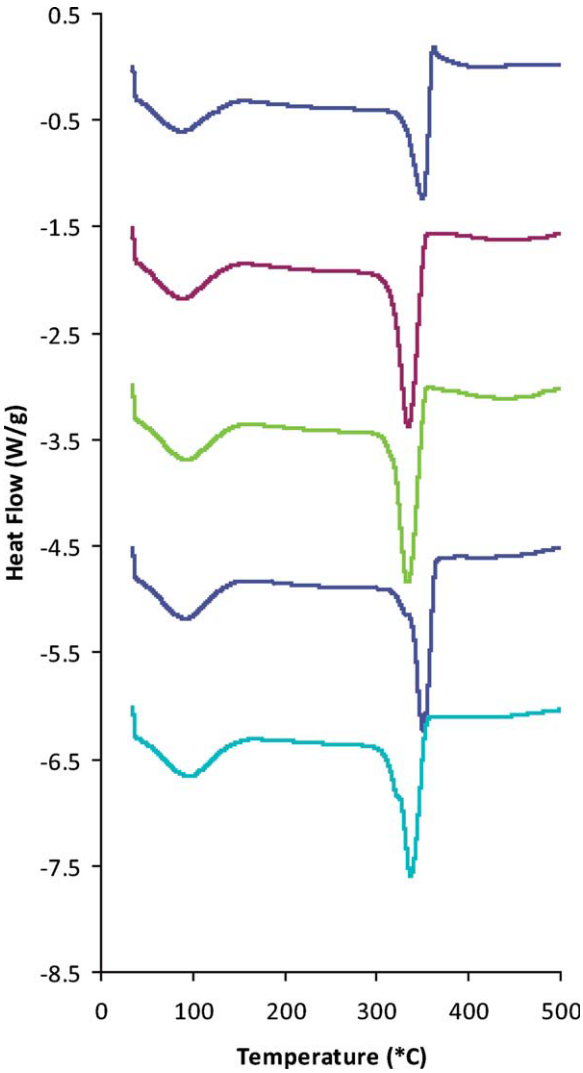


**Figure 7** DSC diagram of control versus plasma-modified samples. [Color figure can be viewed in the online issue, which is available at www.interscience.wiley.com.]

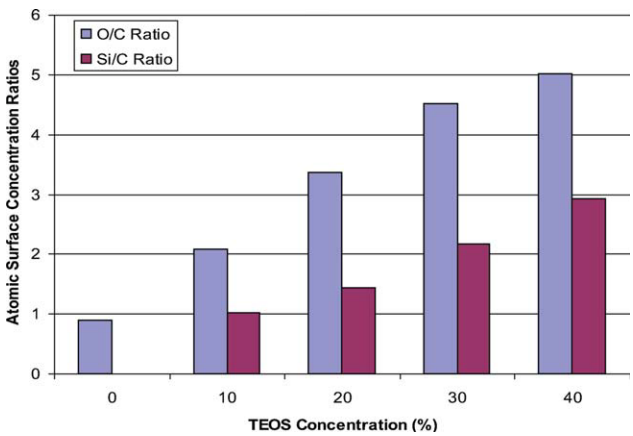


**Figure 8** Relative atomic surface concentration ratios. [Color figure can be viewed in the online issue, which is available at www.interscience.wiley.com.]

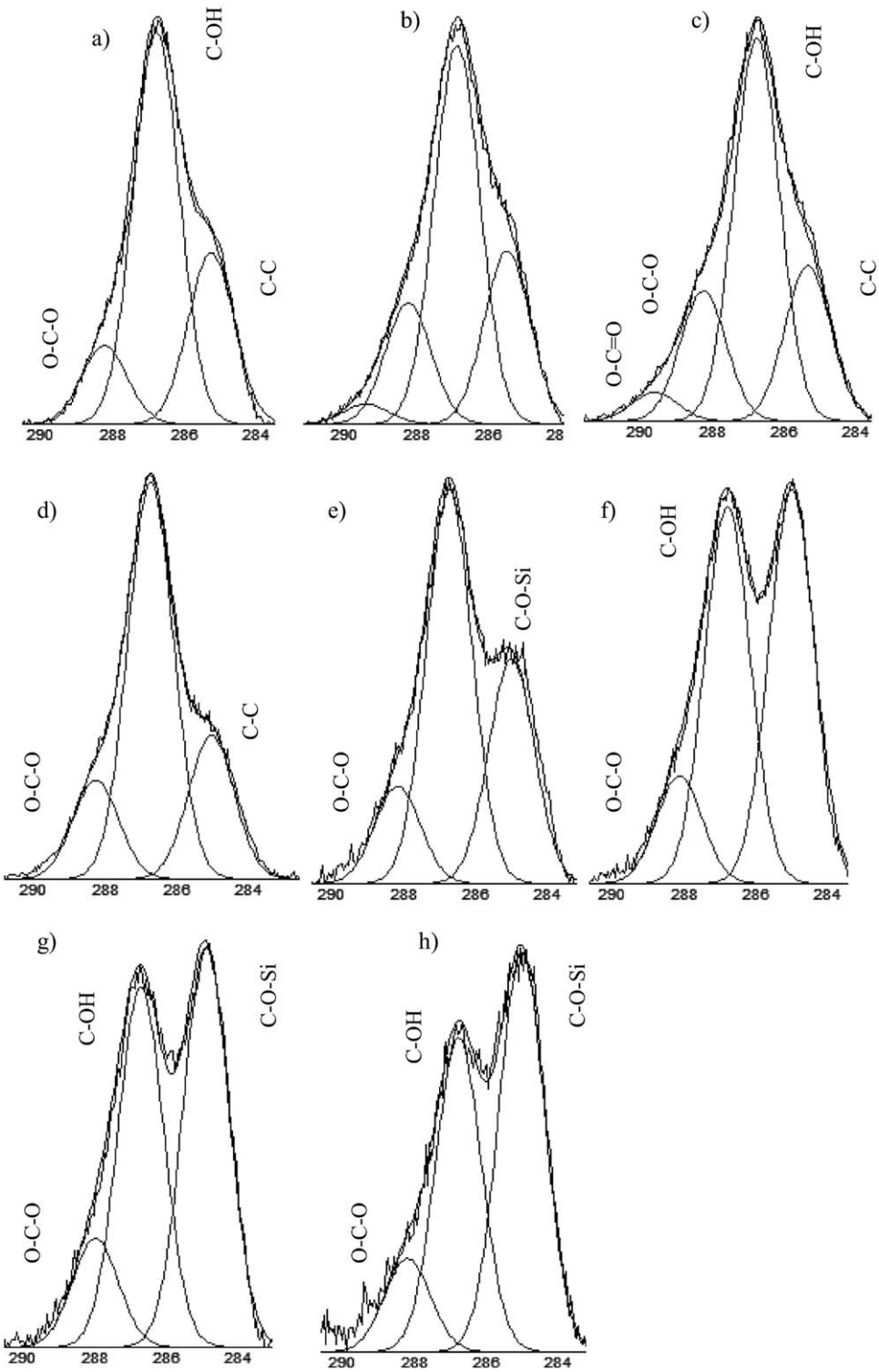


**Figure 9** High resolution C1s spectrum of (a) control extracted cotton (15° take-off angle); (b) APP exposed cotton (15° take-off angle); (c) APP exposed cotton (45° take-off angle); (d) control extracted cotton (45° take-off angle); (e), (f), (g) and (h) $SiO_2$ coated and APP exposed cotton (10, 20, 30, and 40 wt % of TEOS at 45° take-off angle).

surfaces for specific burning spread times. It can be noted that the TEOS concentration was the most influential parameter in the process while the temperature of the solution was less effective. The burning time regression is a quadratic equation with 99.99% chance to express the factors' influences; the power versus time term has been removed due to the statistical low significance. Concentrations of 20–40 wt %,

RF power of 35–80 W and plasma exposure time between 3 and 7 min yield to longer burning spread times. The regression model predicts burning time of 32.26 s for many sets of parameters around 33.7% concentration, 35.5 W RF power, 3.7 min plasma treatment time and 72.7°C TEOS solution temperature [eq. (2)].

$$\begin{aligned} BT = {} & -30.499 + 2.116c + 0.390P + 0.898t + 0.506T \\ & - 4.231 \times 10^{-3}cP + 0.072ct - 2.700 \times 10^{-3}cT \\ & - 2.114 \times 10^{-3}PT - 0.022tT - 0.030c^2 \\ & - 1.312 \times 10^{-3}P^2 - 0.225t^2 - 1.753 \times 10^{-3}T^2 \end{aligned} \quad (2)$$

where BT is burning time (s), $c$ is TEOS concentration (%), $P$ is discharge power (W), $t$ is time (min), and $T$ is temperature of the TEOS solution.

### Thermo gravimetric analysis (TGA)

The thermal behavior of untreated and modified cellulose samples was analyzed in nitrogen atmosphere in a temperature domain of 25–700°C (Fig. 6). The weight-loss processes starts in the 304–316°C temperature range both for the control and $SiO_2$ coated and plasma-treated samples. The weigh-loss decrease of the plasma-treated samples is obvious in comparison with the untreated substrate; the decrease is higher for higher concentrations of the coating solution. At 40 wt % even at temperatures as high as 700°C, the residual weight of nondecomposed substrate present in the system was 25%.

### Differential scanning calorimeter (DSC)

The DSC diagrams of coated (only 30 and 40 wt % TEOS) and plasma-treated cellulose samples show three endothermic processes (Fig. 7). The 50–150°C zone broad peaks are related to loss of water that was probably absorbed by the samples during their processing. Between 315°C and 331°C, the treated samples exhibit a shoulder peak that increases with higher TEOS concentrations. It is assumed that the origin of the shoulder peaks is related to caloric energy induced further condensation (crosslinking)/decomposition reactions of the remaining TEOS in the plasma-modified layers. The peaks in the temperature range of 300–362°C have a thermal effect origin that is also present in nonmodified cellulose at 350°C; however, at a lower intensity comparing to treated samples. The heat enthalpy of the endothermic process (integrating the peaks between 300°C and 362°C) shows an increase for the treated samples (up to 222 J/g) in comparison with control (146 J/g).

### Surface characterization

X-ray photoelectron spectroscopy (XPS)

Results from survey and high resolution (HR) XPS evaluations performed on extracted cellulose, APP exposed cellulose and $SiO_2$ coated and plasma-treated samples are presented in Figures 8 and 9, respectively. According to the diagram in Figure 8, the carbon relative surface atomic concentration of the samples decreases from 24.3% to 11.2% and the silicon atomic concentration increases from 24.9% to

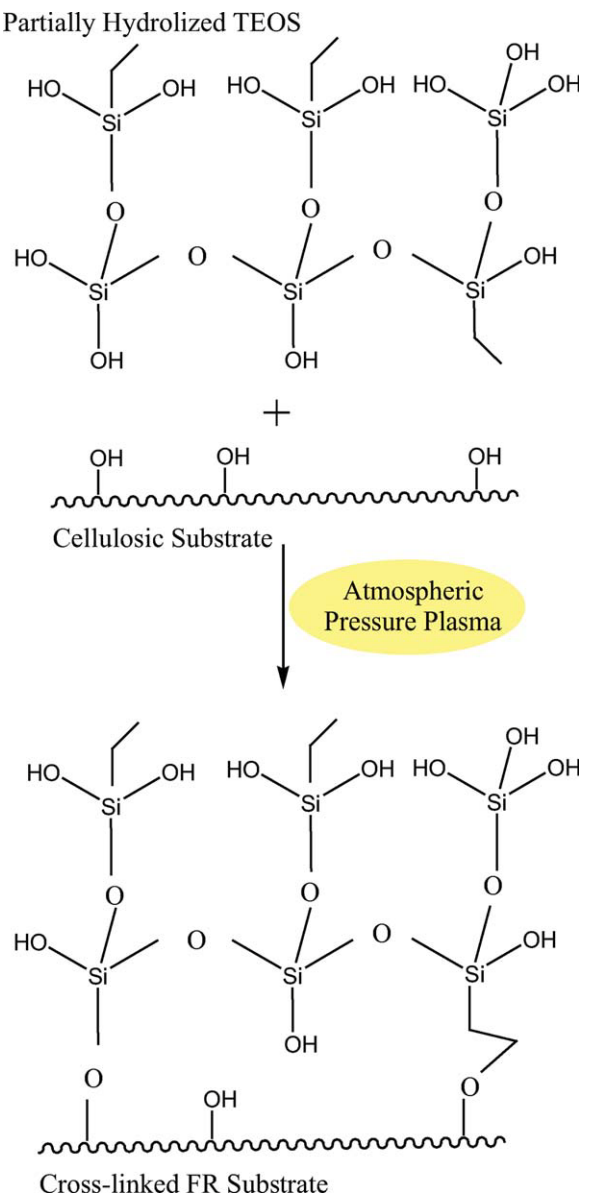


**Figure 10** Suggested APP-induced crosslinking mechanism. [Color figure can be viewed in the online issue, which is available at www.interscience.wiley.com.]

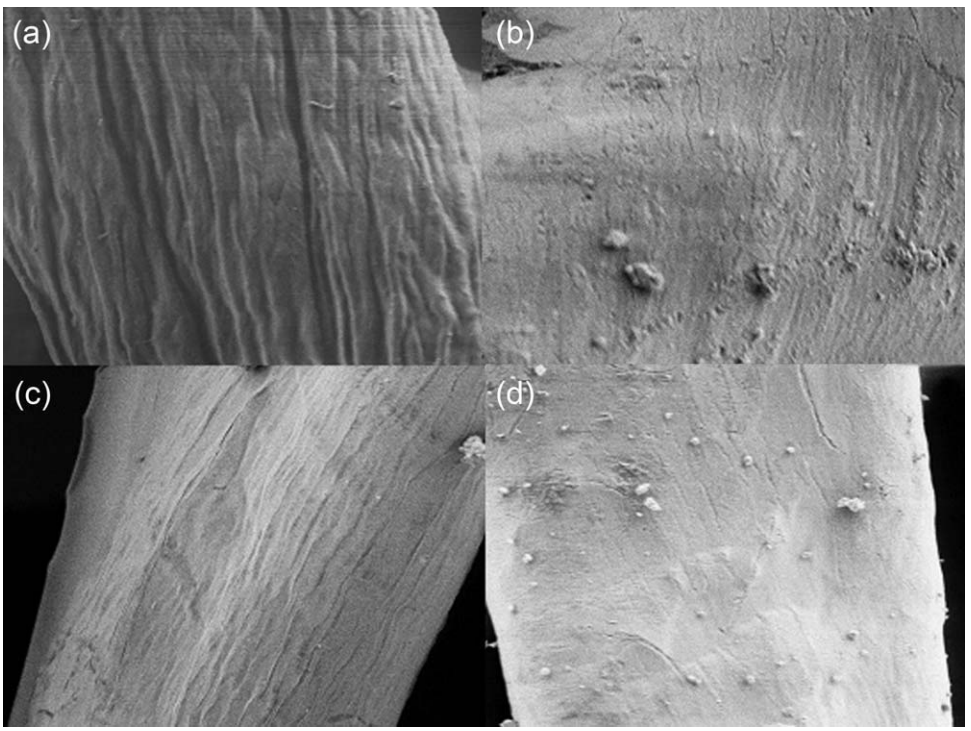


**Figure 11** SEM images of (a) control extracted cotton, (b) SiO2-APP treated cotton (10 wt %), (c) SiO2-APP treated cotton (20 wt %), and (d) SiO2-APP treated cotton (40 wt %).

32.7% as the TEOS concentration increases from 10 to 40 wt %.

HR data collected from clean cellulose samples at 15° take-off angle [Fig. 9(a)] is in agreement with the theoretical relative surface atomic composition of cellulose and with the nature of the surface functionalities.[20,21] It can be observed that even after a 24 h extraction of the cellulose a C—C (285 eV) BE peak is still present in the tri-modal HR diagram, in addition to the existence of C—OH (286.6 eV) and O—C—O (288.2 eV) functionalities. The slightly increased relative carbon surface atomic concentration of the extracted cellulose (64.6%) in comparison with the theoretical value (54.5%) is related to the presence of carbon contamination. However, the relative ratio of the C—OH/O—C—O peak surface areas (61.1/12.2 = 5.0) is very close to the theoretical value (83/17= 4.9).

Similar data collected at 15° take-off angle, from the air-plasma exposed, extracted cellulose [Fig. 9(b)] indicate an increased relative surface oxygen atomic concentration (37.9%) and a significantly modified ratio of the C—OH/O—C—O peak surface areas (54.7/17.4 = 3.1). This allows us to suggest that plasma-induced reaction mechanisms are based on dehydroxylation and O—C—O and O—C=O bond formation reactions.

Plasma-exposed cellulose analyzed at a 45° take-off angle [Fig. 9(c)] exhibits a smaller relative carbon surface atomic concentration (55.2%) and a similar C—OH/O—C—O peak area ratio (2.9) in the tetra modal HR diagram. Accordingly, it can be suggested that the carbon contamination has a surface nature.

Because of the deposition on cellulose fiber surfaces of the $SiO_2$-based layers, the control extracted [Fig. 9(d)] and all coated and plasma-modified substrates [Fig. 9(e–h)] were XPS analyzed at a 45° take-off angle for a deeper evaluation of the surface layers. The control extracted cellulose exhibits a tri-modal pattern, a 4.0 C—OH/O—C—O peak surface area ratio, and a C = 52.8% and O = 47.2% relative surface of carbon and oxygen atomic concentration, respectively.

Results from survey and HR XPS data collected from 10, 20, 30, and 40 wt % TEOS solution coated and air-plasma treated samples [Figs. 8 and 9(e–h)] show a dominant 284.7 eV (C—Si/C—O—Si) BE peak, a decreased carbon and an increased silicon relative surface atomic concentration with the increasing in TEOS concentration of the coating solution. It also should be noted that the ratios of the C—OH/O—C—O peak surface areas do not exhibit a dramatic change (4.1 for 10%, 3.4 for 20%, 3.2 for 30%, and 3.0 for 40% TEOS concentrations). This allows us to suggest that the deposited $SiO_2$ layers on cellulose fiber surfaces were discharge-induced crosslinked and that the bulk of the cellulose substrates was not altered during the plasma process. A suggested plasma-induced crosslinking mechanism of the interface of the $SiO_2$ network with the cellulosic substrate is presented in Figure 10.

Scanning electron microscope (SEM)

The presence of the coating can be easily demonstrated by comparing SEM photomicrograph of a control extracted sample [Fig. 11(a)] with those $SiO_2$-coated (with different concentrations) and APP treated [Fig. 11(b–d)].

As shown in Figure 11(a), the surface morphology along the fiber is wrinkled which contrasts with the treated samples [Fig. 11(b–d)]. The fibers are covered with $SiO_2$ layers demonstrated by the absence of the wrinkled morphology due to the coating and plasma-treatment. It should be noted that the space around the fibers is free of coating [Fig. 11(c,d)], which guarantees the breathability of the fabric.

## CONCLUSIONS

Cotton fibers have been coated with silicone dioxide-based layers using atmospheric pressure plasma (APP) technique. $SiO_2$ network armor was obtained through hydrolysis and condensation of the precursor TEOS and has been crosslinked on the surface of cotton fibers. Because of protection effects of the $SiO_2$ network armor, the modified cellulose fibers exhibit enhanced thermal properties and improved flame retardant. Furthermore, the surface analysis (XPS and SEM) confirm the presence of the $SiO_2$ network on the substrate surfaces even after intense ultrasound washes. $SiO_2$-APP coated textiles could have in the future numerous applications in the development of upholstered furniture, clothing, and military applications.

## References


1. www.cefic-efra.eu (accessed September, 2009).
2. Biron, M. Techniques de l'Ingé nieur 2007, IN77, 2882.
3. Dvornic, P. R.; Jones, R. G.; Ando, W.; Chojnowski, J. Silicon-Containing Polymers; Kluwer Academic Publisher: Netherlands, 2000; p 185.
4. Buch, R. R. Fire Saf 1991, 17, 12.
5. Hshieh, F.-Y. Fire Mater 1998, 22, 69.
6. Quede, A.; Mutel, B.; Supiot, P.; Jama, C.; Dessaux, O.; Delobel, R. Surf Coat Technol 2004, 181, 265.
7. Takao, A.; Kazunori, N. Jpn. Pat. 49,023,278 (1970).
8. Yamaguchi, H. Mokuzai Gakkaishi 1994, 40, 830.
9. Paren, A.; Vapaaoksa, P. U.S. Pat. 5,417,752 (1995).
10. Gutek, B. I. U.S. Pat. 4,419,402 (1983).
11. Mitsuo, I.; Hashimoto, T. Jpn. Pat. 52,063,496 and 54,004,440 (1975).
12. Kuechler, W. L.; Jenkintown, P. U.S. Pat. 3,666,544 (1972).
13. Junichi, K. Jpn. Pat. 49,120,999 (1973).
14. Hideaki, N.; Toshiyuki, I.; Shigeki, Y. Jpn. Pat. 48,091,396 (1972).
15. Park, B. K. WO Pat. 2004,062,815 (2004).
16. Terrance, K. M. GB Pat. 2,290,989 (1996).
17. Totolin, V.; Sarmadi, M.; Manolache, S. O.; Denes, F. S. AATCC Rev 2009, 9, 32.
18. Denes, F. S.; Manolache, S. O.; Hershkowitz, N. U.S. Pat. 6,764,658 B2 (2004).
19. http://www.uni.edu/tapp/pdf%20files/Flame%20Test%20-%2045.pdf (accessed September, 2009).
20. Johansson, L. S.; Campbell, J.; Koljonen, K.; Kleen, M.; Buchert, J. Surf Interface Anal 2004, 36, 706.
21. Mitchell, R.; Carr, C.; Parfitt, M.; Vickerman, J.; Jones, C. Cellulose 2005, 12, 629.